

## Permeation Resistance of Poly(ether ether ketone) to Hydrogen, Nitrogen, and Oxygen Gases

Loxie Monson, Sung In Moon, C. W. Extrand

Entegris, Inc., Chaska, Minnesota 55318

Correspondence to: S. I. Moon (E-mail: sungin\_moon@entegris.com)

**ABSTRACT:** We studied the gas permeation properties of poly(ether ether ketone) (PEEK) and compared it with two other polymers commonly used in the construction of semiconductor microenvironments, polycarbonate (PC), and poly(ether imide) (PEI). The PEEK specimens consisted of extruded films as well as compression- and injection-molded specimens. The compression-molded specimens were prepared to achieve the highest crystallinity. Injection-molded disks, representing products, were milled to a prescribed thickness. Permeation, diffusion, and solubility coefficients were measured on these various PEEK specimens for hydrogen, nitrogen, and oxygen gases. It was found that PEEK generally has better permeation resistance than PC or PEI; showing up to five times lower permeation rates than PC or PEI, depending on grade, crystallinity, and gas. The superior permeation resistance of injection-molded or extruded PEEK, when compared with similarly processed PC or PEI, comes from its crystallinity. © 2012 Wiley Periodicals, Inc. *J. Appl. Polym. Sci.* 000: 000–000, 2012

**KEYWORDS:** poly(ether ether ketones); gas permeation; diffusion; barrier

Received 15 December 2011; accepted 17 February 2012; published online 00 Month 2012

DOI: 10.1002/app.37517

### INTRODUCTION

Silicon (Si) wafers are used for the production of integrated circuits. To protect them from contamination between processing steps, they are stored and transported in special containers called microenvironments (MEs).<sup>1</sup> Polycarbonate (PC) has been widely used in the construction of MEs due to its cleanliness, transparency, toughness, and high softening temperature. However, one drawback of PC is its poor abrasion resistance. Contact between PC and Si wafers during insertion into or removal from MEs can generate unwanted particles.

To minimize particle generation, polymers with superior abrasion resistance are often employed at contact points. Poly(ether ether ketone) (PEEK) often is the material of choice for this task.<sup>2–4</sup> Once PEEK is incorporated, its mass transport properties will influence barrier performance and outgassing properties of the ME product. While the purity and mechanical properties of PEEK are known, its mass transport properties, such as barrier performance and outgassing properties, are not well understood.<sup>5–7</sup> Thus, in this study, we investigated the mass transport properties of PEEK, focusing on how processing and subsequent crystallinity affect permeation.

### ANALYSIS

To analyze the mass transport properties of PEEK and relate them to its morphology, the crystalline percentage ( $x_c$ ) was calculated as<sup>8</sup>

$$x_c = 100 \Delta H / \Delta H_f, \quad (1)$$

where  $\Delta H$  is the measured melting enthalpy and  $\Delta H_f$  is the melting enthalpy of the polymer in a 100% crystalline state.

Gases permeate through homogeneous materials by first dissolving and then diffusing.<sup>9</sup> The downstream pressure rise ( $\Delta p_l$ ) of the permeant can be converted to an equivalent volume of gas ( $V$ ) at standard temperature and pressure

$$V = (\Delta p_l / \Delta p_0)(T_0 / T)V_s, \quad (2)$$

where  $T$  is the measurement temperature,  $V_s$  is the volume of the downstream side of the permeation apparatus,  $T_0$  is standard temperature (32°F = 273 K), and  $\Delta p_0$  is standard pressure (=1 atm or 76 cmHg). The volume ( $V$ ) of gas that permeates through a film with time ( $t$ ) under steady-state conditions depends on the permeability coefficient ( $P$ ), as well as film thickness ( $B$ ), film area ( $A$ ), and the applied upstream pressure ( $\Delta p$ ).<sup>10</sup>

© 2012 Wiley Periodicals, Inc.

$$V = PA\Delta pt/B. \quad (3)$$

The time required for a permeant to break through a film ( $t_b$ ) depends on the film thickness ( $B$ ) and the diffusion coefficient of the material,

$$t_b = B^2/6D. \quad (4)$$

Solubility coefficients were calculated from permeability and diffusion coefficients as

$$S = P/D. \quad (5)$$

## MATERIALS AND METHODS

Victrax<sup>®</sup> Manufacturing Limited supplied two grades of Aptiv<sup>®</sup> extruded films in thicknesses of 50  $\mu\text{m}$  (2 mils), 125  $\mu\text{m}$  (5 mils), and 300  $\mu\text{m}$  (12 mils). According to Victrax, the Aptiv 1000 is more crystalline than the Aptiv 2000. In addition, compression and injection-molded specimens were made at Entegris from Victrax PEEK<sup>™</sup> 150G. Specimens were compression molded using a PHI Bench Design, Hydraulic Compression Press at 350°C (662°F). A specified amount of resin was weighed out for each thickness of film (200  $\mu\text{m}$  (8 mils) and 250  $\mu\text{m}$  (10 mil)), poured into the center of a brass plaque mold, and then sandwiched between polyimide films/thin aluminum sheets. This sandwich was placed on the pre-heated lower platen of the press and brought to a position with the top platen under 2000 lb of force and held until the pressure dissipated, after which the heat was turned off and the sandwich was allowed to cool overnight in the closed position. A 11.4 cm (4½") disk of PEEK 150G was injection molded at Entegris<sup>®</sup> and then sanded on a Timesaver 12S-HPM to the required thickness.

Moreover, we measured the permeation properties of two other ME materials for comparison, PC and poly(ether imide) (PEI). Extruded PC films were obtained from Sabic (8010-MC-112). According to the supplier, the films were extruded from Lexan<sup>®</sup> 141 Bisphenol A PC resin. PEI film specimens were extruded at Ajedim Films using Sabic Innovative Plastics<sup>™</sup> Ultem<sup>®</sup> 1000 resin. Films with thicknesses ( $B$ ) of 250  $\mu\text{m}$  and 510  $\mu\text{m}$  were used.

Melt temperatures ( $T_m$ ), melt enthalpies ( $\Delta H$ ), and crystallization temperatures ( $T_c$ ) of the various films were determined using differential scanning calorimetry (Perkin Elmer<sup>®</sup> Diamond DSC, Waltham, MA). Samples ranging in mass from 4 mg to 8 mg were cut from specimens, heated from 30°C (86°F) to 400°C (752°F), cooled from 400°C to 30°C, and then heated again from 30°C to 400°C at a rate of 10°C/min (18°F/min). Duplicate DSC scans were performed for each material. Using the software resident in the Diamond DSC, the resulting DSC scans were analyzed.

The permeant gases (hydrogen, oxygen, and nitrogen) were industrial grade (hydrogen and nitrogen: >99.9%, oxygen: >99.5%; Toll Co., Minneapolis, MN). The gas permeation apparatus consisted of a sample holder inside of a temperature-controlled chamber, a series of valves, an upstream ballast tank, a pressure transducer (300 psi Heise<sup>®</sup> PM Digital Indicator) for the upstream gas, and a downstream solid-state manometer (10 Torr MKS Baratron<sup>®</sup> Type 627B). The apparatus was constructed from stainless steel. Connections were made by welding or with metal

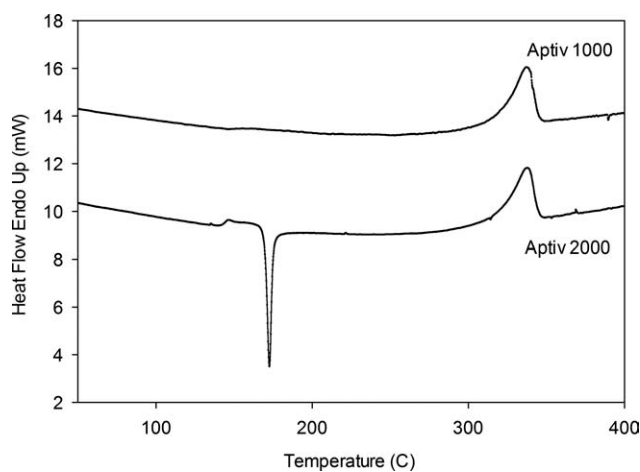


Figure 1. DSC scans of the Aptiv 1000 and 2000 PEEK films.

gasket face seal (Swagelok<sup>®</sup> VCR<sup>®</sup> flanges) to minimize leaks. Data acquisition and control were performed remotely with a personal computer.

Permeation was measured according to standard manometric procedures as described below.<sup>11</sup> A circular specimen with a diameter of 4.6 cm and an effective area ( $A$ ) of 13.7 cm<sup>2</sup> was placed in the gas permeation apparatus. The apparatus was pumped down to ~20 mTorr and held overnight to remove volatile constituents from the apparatus as well as from the specimen. The next day, the apparatus was leak tested. If the leak rate was sufficiently low, then the upstream side of the apparatus was charged with the permeant gas. After pressure and temperatures were allowed to equilibrate for a few minutes, the test was started. The downstream pressure rise ( $\Delta p$ ) was recorded with the passage of time. (Temperature and upstream pressure ( $\Delta p$ ) also were monitored over the duration of the experiment to assure their constancy.) All measurements were made at 25°C (77°F). Measurements were taken from the various thicknesses of each material type using three pressures for each gas: 2, 4, and 6 atm were used for nitrogen and oxygen; 1, 2, and 3 atm were used for hydrogen. Hydrogen measurement was performed at lower pressure than nitrogen and oxygen to adjust the downstream pressure rise rate to an accurately measurable range.

## RESULTS AND DISCUSSION

### Thermal Properties

Thermal properties were measured for each sample type. Figure 1 shows the melting behavior of the extruded films, Aptiv 1000 and 2000. The more crystalline Aptiv 1000 film, shown at the top, had a glass transition temperature ( $T_g$ ) of ~150°C and a peak melt temperature ( $T_m$ ) of ~336°C. The corresponding crystallinity ( $x_c$ ) was calculated from eq. (1) using a  $\Delta H_f$  value of 129 J/g<sup>12</sup>;  $x_c$  values for the Aptiv 1000 films fell between 30% and 32%.

The bottom solid line shows the DSC scan for the more amorphous extruded Aptiv 2000 film. As the PEEK had not fully crystallized during extrusion, two peaks are observed in the DSC scan, a downward peak at ~170°C ( $\Delta H_c$ ) where additional crystal formation occurred and the other, an upward melting peak at ~337°C. A glass transition is also noted at ~150°C.

**Table I.** Overall Averages of Thermal Properties for the Various PEEK Samples<sup>a</sup>

Sample	Process	$T_g$ (°C)	$T_c$ (°C)	$\Delta H_c$ (J/g)	$T_m$ (°C)	$\Delta H_m$ (J/g)	$\Delta H$ (J/g) <sup>b</sup>	$x_c$ (%)
1000	Extruded	152 ± 3	-	-	336 ± 2	38.9 ± 1.2	-	31
2000	Extruded	144 ± 1	172 ± 1	-21.6 ± 0.1	337 ± 1	40.7 ± 1.4	19.1 ± 1.2	15
150G	Compression-molded <sup>c</sup>	148 ± 1 <sup>d</sup>	-	-	345 ± 1	49.4 ± 3.7	-	38
150G	Injection-molded <sup>e</sup>	146 ± 1 <sup>d</sup>	-	-	345 ± 1	34.7 ± 2.5	-	27

<sup>a</sup>The overall averages and standard deviations shown in the table were computed from the individual measurements of all thicknesses, <sup>b</sup>Sum of ( $\Delta H_c + \Delta H_m$ ), according to eq. (6), <sup>c</sup>Compression-molded @ Entegris, allowed to cool overnight in the press under pressure, <sup>d</sup>These glass transition temperatures ( $T_g$ ) were taken from second heating due to weak signal in first heating., <sup>e</sup>Plaque, milled to desired thickness.

In this case, the crystallinity associated with the melting peak is composed of crystallinity that was present from the original extrusion process as well as crystallinity that formed during the heating cycle of the DSC. In order to estimate the fraction of crystallinity in the original sample ( $\Delta H$ ), crystallinity from the heating cycle ( $\Delta H_c$ ) must be subtracted from the crystallinity from the melting peak ( $\Delta H_m$ ). Since the crystallization enthalpy ( $\Delta H_c$ ) is negative and the melting enthalpy ( $\Delta H_m$ ) is positive, numerically  $\Delta H$  can be obtained by summation of  $\Delta H_c$  and  $\Delta H_m$

$$\Delta H = \Delta H_c + \Delta H_m. \quad (6)$$

Crystalline percentage ( $x_c$ ) was calculated from eq. (6) using a  $\Delta H_f$  value of 129 J/g<sup>12</sup>;  $x_c$  values fell between 14% and 16% for the Aptiv 2000 films, about half that of the Aptiv 1000 films.

The compression- and injection-molded specimens showed thermal characteristics similar to the more crystalline Aptiv 1000 films. They had a glass transition temperature ( $T_g$ ) in the vicinity of 146–148°C and a single melting peak at 345°C. Their crystallinity ( $x_c$ ) ranged from 38% to 27%. Overall averages of the thermal properties are listed in Table I for the extruded Aptiv films, along with data for the compression- and injection-molded samples.

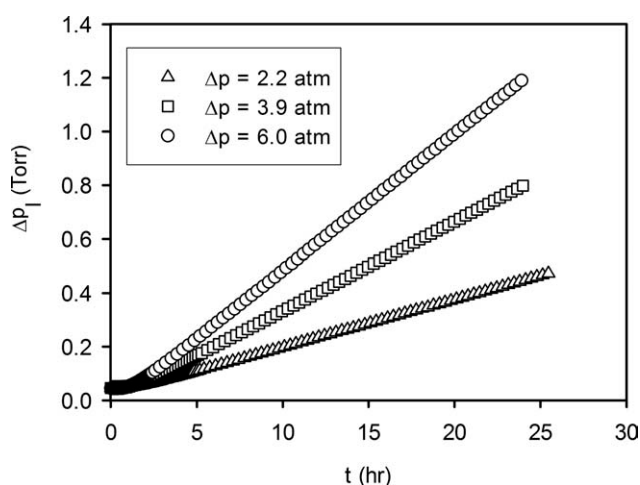


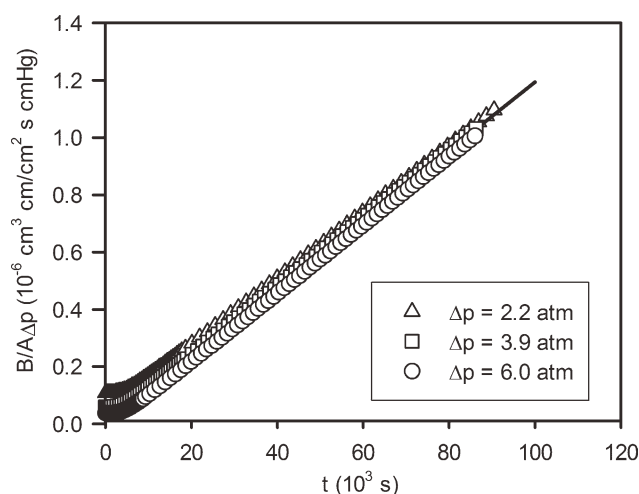
**Figure 2.** Downstream pressures ( $\Delta p_1$ ) versus time ( $t$ ) of a 0.13 mm crystalline PEEK film (Aptiv 1000) for oxygen gas at various upstream pressures ( $\Delta p$ ).

The various types of PEEK showed quite different melting behavior and crystalline content, demonstrating that crystallinity is greatly affected by process conditions. The 150G film compression molded at Entegris had higher crystallinity (38%) than Aptiv 1000 film. The more crystalline extruded Aptiv 1000 film and the injection-molded plaque had similar crystalline content, around 30%. The extruded Aptiv 2000 films had the lowest crystallinity, about 15%. The differences are almost certainly due to variation in cooling rates from one process to the next.

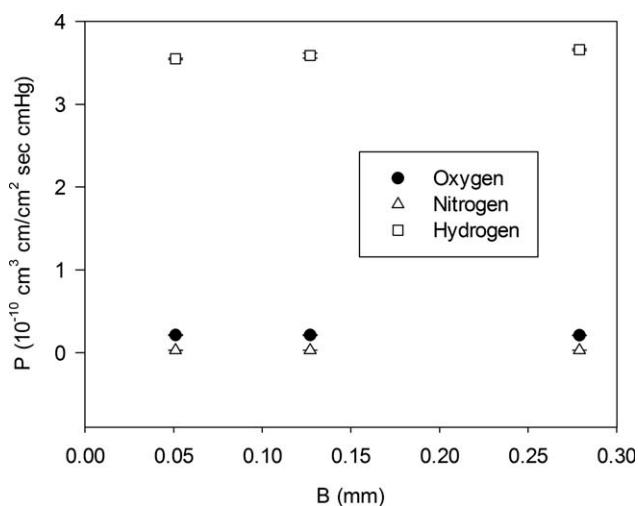
### Permeation

Figure 2 shows downstream pressure ( $\Delta p_1$ ) versus time for oxygen permeating through a 0.13 mm PEEK film at various upstream pressures ( $\Delta p$ ). Initially, the downstream pressure remained the same. Once oxygen broke through the sample, the downstream pressure rose and reached a steady state. Permeation rates were proportional to the applied upstream pressure and inversely proportional to the thickness.

The downstream pressures ( $\Delta p_1$ ) from Figure 2 were converted to gas volumes at standard temperature and pressure [eq. (2)] and then plotted in Figure 3 as  $VB/A\Delta p$  versus  $t$  according to eq. (3). The points are experimental data. The solid line represents linear regression for longer times. The slope of the line in Figure 3 equates to the permeability coefficient ( $P$ ), which, for this film, has a value of  $P = 0.1 \times 10^{-10} \text{ cm}^3 \text{ cm/cm}^2 \text{ s cmHg}$ . The



**Figure 3.** A plot of  $VB/A\Delta p$  versus time ( $t$ ) for oxygen permeating through a 0.13 mm crystalline PEEK film (Aptiv 1000) at various upstream pressures ( $\Delta p$ ).



**Figure 4.** Permeability coefficients ( $P$ ) of oxygen, nitrogen, and hydrogen through amorphous PEEK films (Aptiv 2000) of various thickness ( $B$ ).

break-through times ( $t_b$ ) were estimated from the intersection of two lines—the first is defined by the permeability coefficient and the second is a zero slope line passing through the initial  $\Delta p$  at  $t = 0$  s. The average break-through time for this film was  $t_b = 1.4$  h, corresponding to  $D = 0.5 \times 10^{-8} \text{ cm}^2 \text{ s}^{-1}$ . Combinations of the various gases and PEEK materials behaved similarly. Given the uncertainty of the temperature, the pressures, the downstream volume, and the dimensions of the polymer specimen, the uncertainty of our  $P$  value measurement was generally less than 5%.  $D$  value has higher uncertainty due to additional calculation of break-through time using intersection.

Figure 4 shows permeability coefficients ( $P$ ) of the three gases through the amorphous PEEK films as a function of thicknesses ( $B$ ). The permeability coefficients were largely independent of film thickness. This was also true for the other types of PEEK films. Thus, the data from the various pressures and thicknesses gave unique values of  $P$ ,  $D$ , and  $S$ . Tables II–IV summarize the mass transport coefficients for the three different gases. Overall averages showed that due to the slower cooling rate, the Entegris compression-molded film had the best permeation resistance to all gases, almost three times better than the 2000 series.

**Table III.** Overall Averages of Permeability Coefficients ( $P$ ), Diffusion Coefficients ( $D$ ), and Solubility Coefficients ( $S$ ) of the Nitrogen Gas for the PEEK Films at 25°C (77°F)<sup>a</sup>

Sample	$P$ ( $10^{-10}$ $\text{cm}^3 \text{ cm/cm}^2 \text{ s}$ $\text{cmHg}$ )	$D$ ( $10^{-8}$ $\text{cm}^2 \text{ s}^{-1}$ )	$S$ ( $10^{-3}$ $\text{cm}^3/\text{cm}^3$ $\text{cmHg}$ )
1000	$0.016 \pm 0.001$	$0.127 \pm 0.009$	$1.28 \pm 0.07$
2000	$0.030 \pm 0.001$	$0.212 \pm 0.011$	$1.41 \pm 0.06$
150G compression	$0.011 \pm 0.001$	$0.106 \pm 0.011$	$1.04 \pm 0.09$
150G injection	$0.017 \pm 0.002$	$0.189 \pm 0.030$	$0.93 \pm 0.09$

<sup>a</sup>Total overall averages and standard deviations shown in the table were computed from the individual measurements of all thicknesses at all pressures.

**Table II.** Overall Averages of Permeability Coefficients ( $P$ ), Diffusion Coefficients ( $D$ ), and Solubility Coefficients ( $S$ ) of the Hydrogen Gas for the PEEK Films at 25°C (77°F)<sup>a</sup>

Sample	$P$ ( $10^{-10}$ $\text{cm}^3$ $\text{cm/cm}^2$ $\text{s cmHg}$ )	$D$ ( $10^{-8}$ $\text{cm}^2 \text{ s}^{-1}$ )	$S$ ( $10^{-3}$ $\text{cm}^3/\text{cm}^3$ $\text{cmHg}$ )
1000	$1.81 \pm 0.25$	$29.6 \pm 3.4$	$0.61 \pm 0.04$
2000	$3.60 \pm 0.05$	$53.2 \pm 6.4$	$0.69 \pm 0.09$
150G compression	$1.16 \pm 0.04$	$24.2 \pm 4.9$	$0.50 \pm 0.10$
150G injection	$2.01 \pm 0.04$	$51.6 \pm 2.8$	$0.39 \pm 0.02$

<sup>a</sup>Total overall averages and standard deviations shown in the table were computed from the individual measurements of all thicknesses at all pressures.

As with other materials, hydrogen permeated faster than oxygen and nitrogen, primarily due to its smaller molecular size.<sup>13</sup>

Figure 5 shows the relation between the mass transport properties of PEEK for oxygen and its crystallinity. The black square points are the average values of the 1000 and 2000 films. Other points (circles and triangles) are other average values listed in Table IV. The solid lines in each plot were fitted through the two points representing the 1000 and 2000 films.

$P$  values decreased with crystalline content of the PEEK. According to Nielsen,<sup>14</sup> for impermeable spherical particles, the permeability should vary linearly with the fraction of the impermeable particles. If we assume the crystalline domains that are relatively impenetrable and have spherical proportions (or at least have an aspect ratio of  $\sim 1$ ), then a linear relation is expected and indeed produced a reasonable fit of the data.

$D$  values also decreased linearly with  $x_c$ , but showed more scatter than  $P$  values. Diffusion coefficients are especially sensitive to crystalline structure since differences in the paths would result in different travel times. Thus, in addition to variation in overall crystalline content, it appears that there also may have been differences in morphology.

In contrast to  $P$  and  $D$ ,  $S$  values appear to vary in a nonlinear fashion.  $S$  values were calculated from the  $P/D$  ratio, so  $S$  values were not primary measurement from the raw data. Any

**Table IV.** Overall Averages of Permeability Coefficients ( $P$ ), Diffusion Coefficients ( $D$ ), and Solubility Coefficients ( $S$ ) of the Oxygen Gas for the PEEK Films at 25°C (77°F)<sup>a</sup>

Sample	$P$ ( $10^{-10}$ cm <sup>3</sup> cm/cm <sup>2</sup> s cmHg)	$D$ ( $10^{-8}$ cm <sup>2</sup> s <sup>-1</sup> )	$S$ ( $10^{-3}$ cm <sup>3</sup> /cm <sup>3</sup> cmHg)
1000	0.107 ± 0.016	0.473 ± 0.144	2.37 ± 0.45
2000	0.212 ± 0.004	0.803 ± 0.041	2.64 ± 0.15
150G compression	0.078 ± 0.004	0.405 ± 0.063	1.93 ± 0.25
150G injection	0.123 ± 0.016	0.841 ± 0.033	1.46 ± 0.14

<sup>a</sup>Total overall averages and standard deviations shown in the table were computed from the individual measurements of all thicknesses at all pressures.

fluctuation from  $P$  or  $D$  values would have been augmented in the  $S$  values, especially fluctuation from the  $D$  values. Separate measurements, such as a sorption test, would be needed to improve our understanding of the relation between solubility and crystallinity.

If extrapolated to zero crystallinity, we obtain an estimate of the mass transport properties of completely amorphous PEEK. Zero crystallinity values of  $P$  were as much as five times greater than values for the most crystalline versions of PEEK. Values of amorphous PEEK ( $x_c = 0\%$ ) are listed in Table V along with values from PC and PEI, two other amorphous polymers commonly used in ME applications. PEEK values are estimated at zero crystallinity, and PC and PEI values were measured in this study. While the  $D$  and  $S$  values of the various amorphous poly-

mers were of the same order of magnitude, the  $P$  values of PEEK and PEI were surprisingly similar. At the molecular level, both have a rigid backbone dominated by aromatic linkages. Alternatively, the PC, which has a more flexible chain with a mixture of aliphatic and aryl linkages, had a larger permeability.

In standard polymer processing, such as injection molding or extrusion, a perfectly amorphous PEEK sample would be difficult to produce. From our findings, one could conclude that the superior permeation resistance of injection-molded or extruded PEEK, when compared with similarly processed PEI, comes from its crystallinity.

## CONCLUSIONS

Permeability, diffusion, and solubility coefficients were measured for various different PEEK films and were found to be independent of applied upstream pressure and thickness. Compression-molded and annealed samples allowed to cool in the press overnight produced higher crystallinity and greater permeation resistance than the extruded films supplied by Victrex. Slower cooling

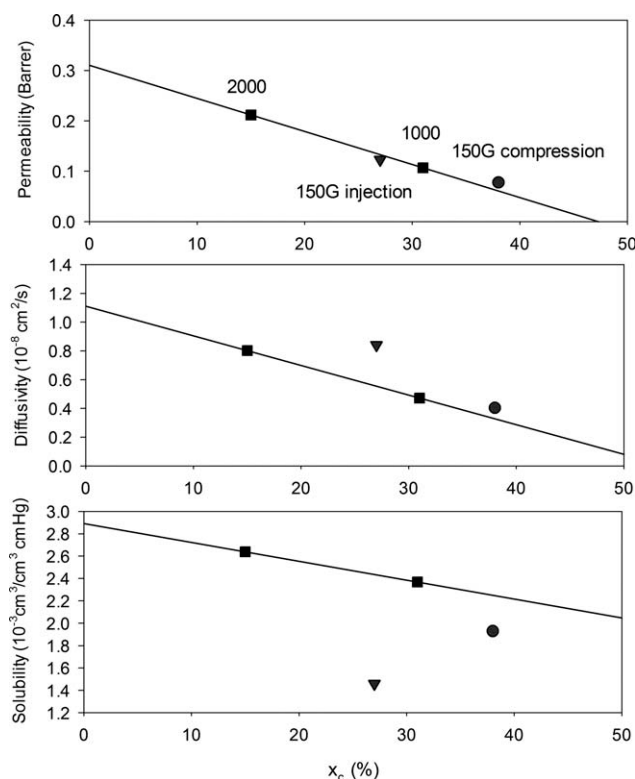


**Figure 5.** Permeability coefficients ( $P$ ) (Barrer =  $10^{-10}$  cm<sup>3</sup> cm/cm<sup>2</sup> s cmHg), diffusion coefficients ( $D$ ), and solubility coefficients ( $S$ ) versus crystallinity ( $x_c$ ) for oxygen.

**Table V.** Permeability Coefficients ( $P$ ), Diffusion Coefficients ( $D$ ), and Solubility Coefficients ( $S$ ) of all Gases for the Amorphous PEEK<sup>a</sup> at 25°C (77°F) When Compared with Amorphous PEI<sup>b</sup> and PC<sup>b</sup>

Gas	Polymer	$P$ ( $10^{-10}$ cm <sup>3</sup> cm/cm <sup>2</sup> s cmHg)	$D$ ( $10^{-8}$ cm <sup>2</sup> s <sup>-1</sup> )	$S$ ( $10^{-3}$ cm <sup>3</sup> /cm <sup>3</sup> cmHg)
H <sub>2</sub>	PEEK	5.28	75.3	0.765
	PEI	6.04	52.4	1.18
	PC	10.6	153	0.723
N <sub>2</sub>	PEEK	0.043	0.292	1.53
	PEI	0.037	0.11	3.41
	PC	0.24	1.28	1.92
O <sub>2</sub>	PEEK	0.310	1.11	2.89
	PEI	0.297	0.58	5.19
	PC	1.18	3.53	3.36

<sup>a</sup>Amorphous PEEK values were calculated using extrapolation of data in Figure 5 to zero crystallinity for oxygen and the same methods were used for nitrogen and hydrogen, <sup>b</sup>PEI and PC values were measured in this study as discussed in experimental section.

rates associated with the press-cooled specimen generally led to greater crystallinity and better permeation resistance. By extrapolating the PEEK data to a completely amorphous state, or 0% crystallinity, we found that there was correlation with the permeability rate of PEI, which has a chemical structure similar to that of PEEK. The same could not be said of the diffusivity or solubility.

## REFERENCES

1. Extrand, C. W. *Semiconductor Fabtech* **2008**, 3, 43.
2. Bhatt, S. *Micro* **1999**, 17, 37.
3. Extrand, C. W.; Bhatt, S. *J. Mater. Sci.* **2000**, 35, 5427.
4. Moon, S. I.; Monson, L. L.; Extrand, C. W. *J. Appl. Polym. Sci.* **2006**, 102, 2362.
5. Handa, Y. P.; Roovers, J.; Moulinie, P. *J. Polym. Sci. Part B: Polym. Phys.* **1997**, 35, 2355.
6. Kumazawa, H.; Wang, J.-S.; Fukuda, T.; Sada, E. *J. Membr. Sci.* **1994**, 93, 53.
7. Orchard, G. A. J.; Ward, I. M. *Polymer* **1992**, 33, 4207.
8. Runt, J. P. In *Encyclopedia of Polymer Science and Engineering*; Kroschwitz, J. I., Ed.; Wiley: New York, **1986**; Vol. 4, pp 487.
9. Osswald, T. A.; Menges, G., *Materials Science of Polymers for Engineers*; Hanser: New York, **1995**.
10. Crank, J. *The Mathematics of Diffusion*; Oxford University Press: London, **1970**.
11. ASTM D1434-82. Standard Test Method for Determining Gas Permeability Characteristics of Plastic Film and Sheeting, ASTM: West Conshohocken, PA, **1998**. See also JIS K7126.
12. Blundell, D. J.; Osborn, B. N. *Polymer* **1993**, 24, 953.
13. Vieth, W. R. *Diffusion in and Through Polymers*; Hanser: New York, **1991**.
14. Nielsen, L. E. *J Macromol Sci Chem* **1967**, A1, 929.